

Raman study of the nitrided GaAs thin layers

Eui Kwan Koh*

Department of Physics, Korea University, Seoul 136-701, Korea

Young Ju Park, Eun Kyu Kim, and Suk-Ki Min

Semiconductor Materials Laboratory, Korea Institute of Science and Technology, P.O. Box 131, Cheongryang, Seoul 130-650, Korea

Sung Ho Choh

Department of Physics, Korea University, Seoul 136-701, Korea

(Received 29 December 1997)

The properties of the nitrided GaAs thin layers have been investigated by using Raman spectroscopy. The nitrided GaAs thin layers were prepared by irradiating electron-cyclotron resonance (ECR) nitrogen plasma at various substrate temperatures from room temperature to 600 °C. Raman measurements have shown that not only are the longitudinal-optical (LO) and transverse-optical (TO) phonon modes shifted down in frequency, but also the LO-TO splitting decreases as the nitridation temperature increases. It is believed that the origin of the frequency shifts is the changes in effective charge and the strain effects due to defects included in the nitrided GaAs thin layers. The bandwidth for the LO-phonon mode for the sample nitrided at 600 °C is the largest, which means that the nitridation at high temperature causes more disordered surface structure. We have estimated several physical parameters in the nitrided GaAs thin layers, such as the fraction of defects, the strains, and the correlation length from the measured Raman spectra. [S0163-1829(98)05719-1]

I. INTRODUCTION

Nitridation technique has been used for the formation of a thin nitrided buffer layer on which high-quality nitrided films can be formed.¹ Particularly, this technique is one of the important processes for the growth of GaN layer, which is considered to be the most promising semiconducting materials for optical devices in the spectral region from blue to ultraviolet light.^{2,3} Also, it makes use of the formation of a thin nitrided GaAs for a passivating layer that is applicable to the mask material for selective area growth of GaAs.⁴ Several nitridation techniques have been reported, high-temperature annealing (above approximately 600 °C) in NH₃ or N₂, N⁺-ion bombardment, and plasma or photon-assisted decomposition of N₂ (or NH₃) were employed to form nitrided films.⁵ To obtain reactive N species at lower annealing temperature, several precursors such as N₂H₄ and N₂H₂(CH₃)₂ have also been reported.⁶

Raman scattering by photons provides valuable information on many physical properties of crystals. Moreover, when the photon energies lie in the vicinity of electronic absorption bands of semiconductors, the electronic structure of the crystal becomes an important part in the Raman process. So, Raman scattering technique has been a powerful tool for studying the electronic⁷ and lattice dynamic properties⁸ of semiconductor superlattices, to characterize the crystalline quality of epitaxial layers, and to study the interfacial strains⁹⁻¹² in heterostructures. Their sensitivity to vibronic and electronic properties allows us to access the improvement of growth conditions. The Raman studies in relation to semiconductors have mainly concentrated on the bulk materials and the epitaxial layers. There have also been studies of the surface damage by ion implantation, which causes great damage to the surface and generates large strains. However, studies on thin nitrided layers have rarely been reported because the surface modification of the nitri-

dation causes much smaller strains compared to that of the ion implantation. So it is difficult to detect the scattered light from the near-surface region by the conventional Raman measurement because the thickness of the nitride layer is limited within a few tens nm from the surface.

In this work, we have investigated the properties of the thin nitrided GaAs layer by Raman scattering. In order to make the surface measurement sensitive, we adopted an oblique forward Raman scattering geometry ($\theta \cong 160^\circ$). We have also estimated several physical parameters, such as the fraction of defects, the strains, and the correlation length from the measured Raman spectra. Particularly, this work is mainly concentrated on the study of defects in the nitrided films based on the obtained physical parameters.

II. EXPERIMENT

The nitridation process by plasma irradiation on the GaAs surfaces was performed in an ultrahigh-vacuum (UHV) chamber fitted with an ECR plasma source.¹³ The sample used in this study was an n^+ GaAs (001) wafer with about $2 \times 10^{18} \text{ cm}^{-3}$ carrier concentrations. Nitridation was performed at various substrate temperatures in the UHV system on the hydrogen plasma cleaned (001) surface, after heating the sample to N₂ plasma exposure temperature. The nitridation conditions of the prepared samples are summarized in Table I. Raman measurements were performed at room temperature. The 514.5 nm line of an Ar⁺ ion laser was used as an exciting source. The laser power used was about 200 mW. The scattered light was dispersed by a 1 m double monochromator with 1800 line/mm gratings (Jasco NR1100), and the signal was detected with a photomultiplier tube (PMT) operated in the photon counting mode. The penetration depth l of the light is proportional to $(\alpha_i + \alpha_s)^{-1}$, where $\alpha_{i(s)}$ is the absorption coefficient for the incident (scattered) light. It is expected that the penetration depth l is about 100 nm at

TABLE I. Conditions of preparing thin nitrided GaAs samples.

Sample name	Substrate temperature (°C)	Nitridation time (min)	Plasma power (W)	Chamber pressure (Torr)
RT	RT			
T100	100			7×10^{-4}
T300	300	30	100	(10 sccm of nitrogen gas)
T450	450			
T550	550			
T600	600			

514.5 nm.¹⁴ The nitrided thickness is only a few tens nm in depth.¹³ In order to obtain more information from the near surface region, we adopted an oblique forward scattering geometry ($\theta \cong 160^\circ$) (see the inset of Fig. 1). In such geometry, the penetration depth is expected to be approximately 30 nm, which is similar to the depth of the nitrided layer. Hence, we can obtain the Raman spectra from the near-surface nitrided layer rather than from the bulk region that is located deep inside the nitrided sample.

III. RESULT AND DISCUSSION

GaAs has two first-order Raman bands, namely, TO- and LO-phonon bands. Only the LO-phonon band is allowed by the Raman selection rule from the (001) face of a zincblende-type crystal, and the TO-phonon band is allowed only when the thin layer on (001)GaAs contains misoriented regions. Figure 1 shows the unpolarized Raman spectra taken from the samples nitrided at various temperatures. As can be seen in Fig. 1, both the LO and TO bands are observed in the un-nitrided and the nitrided samples and the peak height ratio of TO/LO is distributed in the range from 0.4 to 0.6 for each sample. These indicate that the samples used in this work consist of small grains with somewhat random crystallographic orientation. In addition, the shape and position for

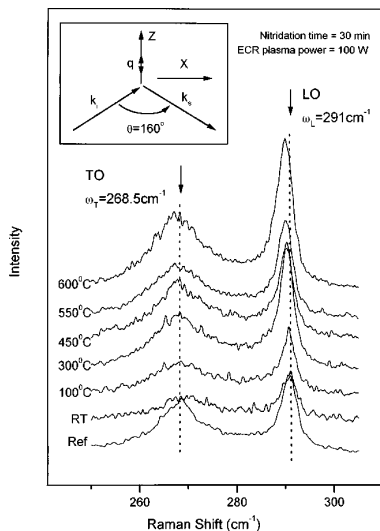


FIG. 1. Unpolarized Raman spectra measured at room temperature. Arrows indicate the LO phonon ($\omega_L = 291.0 \text{ cm}^{-1}$) and the TO phonon ($\omega_T = 268.5 \text{ cm}^{-1}$) frequencies. The inset is an oblique forward scattering diagram of the experiment. The wave-vector directions of the incident and scattered photons are indicated by k_i and k_s , respectively, and that of the phonon is indicated by q .

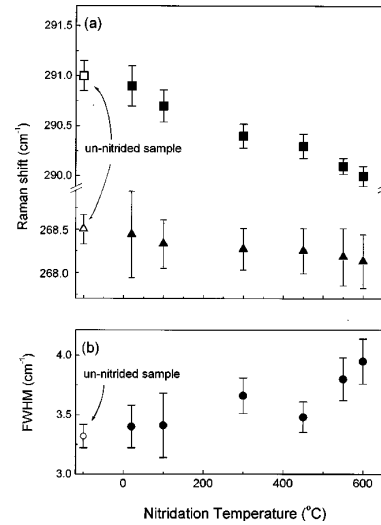


FIG. 2. (a) LO-phonon (■) and TO-phonon (▲) Raman frequencies and (b) the FWHM (full width at half maximum) (●) for the LO phonon determined by fitting the Lorentzian line shape to the Raman spectra in Fig. 1.

both bands show slight differences between the nitrided and the un-nitrided samples, which are related to the existence of defects. These slight changes can be distinguished by Lorentzian fitting. Figure 2 shows the dependence of the LO and TO bands as a function of nitridation temperature with respect to the results obtained by the Lorentzian fitting for each sample. The peak frequency of the LO and the TO phonon and the bandwidth for the LO phonon are shown in Figs. 2(a) and 2(b), respectively. It is worth noticing that the LO and TO bands are downshifted according to the increasing nitridation temperature. While the LO bandwidths of the nitrided samples are broader as a function of temperature than that of the un-nitrided sample [see Fig. 2(b)], the TO bands do not show any tendency for the line broadening (not shown here). The downshift of LO- and TO-phonon frequency may be explained in terms of crystalline defects,^{15,16} the change in lattice constant,⁹⁻¹² the mass difference, and the reduction in the effective charge.¹⁷ The broadening of the Raman peak takes into account regarding these effects; the anharmonic effect due to the phonon-phonon interaction or the relaxation of the q -selection rule arising from the vanishing periodicity.^{18,19} Being based upon these facts, we can estimate several physical parameters, such as the fraction of defects, the strain, and the correlation length.

Since the small amounts of the injected nitrogen exist sparsely in layers within approximately 30 nm from the surface, the lattice distortions in each single layer may exist in the nitrided region. So a tensile stress may be expected in the nitrided GaAs thin layer due to a tetragonal lattice distortion. Thus, the threefold degenerated optic modes (T_d point symmetry) are split into a singlet (ω_s) with an eigenvector parallel to the stress and two doublets (ω_d) with eigenvectors perpendicular to the stress.^{11,12} The shifts of the phonon frequencies for the singlet and the doublet are given by

$$\begin{aligned} \Delta \omega_s &= \omega_s - \omega_0 = \Delta \omega_H + \frac{2}{3} \Delta \omega, \\ \Delta \omega_d &= \omega_d - \omega_0 = \Delta \omega_H - \frac{1}{3} \Delta \omega, \end{aligned} \quad (1)$$

where

$$\Delta \omega_H = (\sigma/6\omega_0)(p+2q)(S_{11}+2S_{12}),$$

TABLE II. Dimensionless values p and q of phonon deformation potentials for LO and TO phonons, and elastic compliance constants S_{11} and S_{12} (in units of 10^{-12} dyn $^{-1}$ cm 2) for GaAs (from Ref. 11).

$S_{11} + 2S_{12}$	0.445
$S_{11} - S_{12}$	1.54
$[(p-q)/\omega^2]_{\text{LO}}$	0.7 ± 0.03
$[(p-q)/\omega^2]_{\text{TO}}$	0.3 ± 0.03
$[-(p+2q)/6\omega^2]_{\text{LO}}$	1.23 ± 0.03
$[-(p+2q)/6\omega^2]_{\text{TO}}$	1.11 ± 0.03

$$\Delta\omega = (\sigma/2\omega_0)(p-q)(S_{11}-S_{12}), \quad (2)$$

where S_{ij} are the elastic compliance constants, and p and q are the constants describing the changes in the spring constant due to the stress. The values used in this calculation are listed in Table II.

One problem encountered with an experiment having an oblique forward scattering configuration was the mixing of the backward scattering configuration. Such mixing was produced mainly by the first reflected beam from the back and the front surface inside the material, respectively. As a result, both the singlet and the doublet can affect the TO and LO phonons. Hence the strain σ along (100) for the oblique forward scattering produces the LO- or TO-phonon frequency shift $\Delta\omega_s + \Delta\omega_d$.⁹ By substituting the values of Table II into Eqs. (1) and (2), the frequency shifts of LO ($\Delta\omega_L$) and TO ($\Delta\omega_T$) phonons are expressed as

$$\begin{aligned} \Delta\omega_L &= -2.65\sigma \text{ GPa}^{-1}, \\ \Delta\omega_T &= -2.44\sigma \text{ GPa}^{-1}, \end{aligned} \quad (3)$$

respectively. If the experimental uncertainty is included, there is almost no difference between the shifts of the LO and TO phonons. Hence the strain effect would tend to reduce equally both the LO and the TO frequencies. Since the frequency shift of the TO phonon of the sample T600 from the un-nitrided sample is about 0.37 cm^{-1} , the magnitude of the stress is estimated to be $\sigma \approx 0.15 \text{ GPa}$.

The reduction in effective charge also causes the shift of the Raman peak. Since the strain in layers causes both the LO and TO phonons with no difference, however, the shift of the LO phonon being much bigger than that of the TO phonon, it indicates that the reduction of the electric field associated with the LO phonon is the major effect. According to the XPS (x-ray photoelectron spectroscopy) measurement,¹³ the thin nitrided GaAs layers consisted in a composition of $\text{GaAs}_{1-x}\text{N}_x$. The substitutions of N for As result in the change of the effective charge and the mass reduction. The resulting expression for the LO-TO splitting becomes¹⁷

$$(\omega_L^2 - \omega_T^2)/(\omega_{\text{LO}}^2 - \omega_{\text{TO}}^2) = (1-x)^2/(1-0.392x), \quad (4)$$

where $\omega_{\text{LO}} = 291.0 \text{ cm}^{-1}$ and $\omega_{\text{TO}} = 268.5 \text{ cm}^{-1}$ are the LO- and TO-phonon frequencies, respectively.

Substituting the experimental results of Fig. 2 into Eq. (4), we can estimate the fraction x (%) of substituted nitrogen atoms, which is found to be in the range from 0.05% to 1.8%

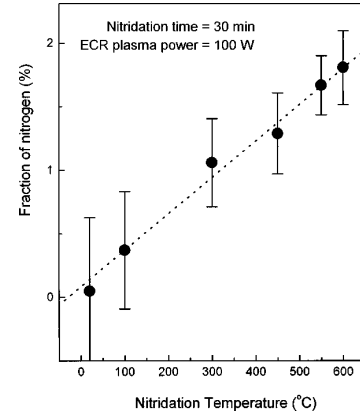


FIG. 3. The fraction (x) of As sites substituted by N from the LO-TO splitting. The dotted line is the linear fitting result.

as shown in Fig. 3. The dotted line is a linear fit, indicating that the amount of the nitrogen increases linearly with the nitridation temperature.

A “spatial correlation” model with a Gaussian correlation function is general and makes it possible to use Raman spectra to evaluate an average size of undamaged regions in semiconductors.^{18,19} By assuming that the finite size of the correlation regions in the damaged material is a sphere, the Raman intensity, $I(\omega)$, at a frequency ω , can be written as

$$I(\omega) \propto \int_0^1 \exp(-q^2 L^2/4) (d^3q) / \{[\omega - \omega(q)]^2 + (\omega_0/2)^2\}, \quad (5)$$

where q is expressed in units of $2\pi/a_l$, a_l is the lattice constant, L is the spatial correlation length, and ω_0 ($= 3.32 \text{ cm}^{-1}$) is the bandwidth of the unperturbed Raman line shape for the un-nitrided sample. For the dispersion $\omega(q)$ of the LO phonon we take the analytical relationship based on a one-dimensional linear-chain model,¹⁹

$$\omega^2(q) = A + \{A^2 - B[1 - \cos(\pi q)]\}^{1/2}, \quad (6)$$

where $A = 4.23 \times 10^4 \text{ cm}^{-2}$ and $B = 7.11 \times 10^8 \text{ cm}^{-4}$ for the un-nitrided GaAs. Figure 4 shows the relationship between the Raman shift of LO phonon $\Delta\omega_{\text{LO}}$ and the broadening ω as a function of correlation length as determined from Eqs.

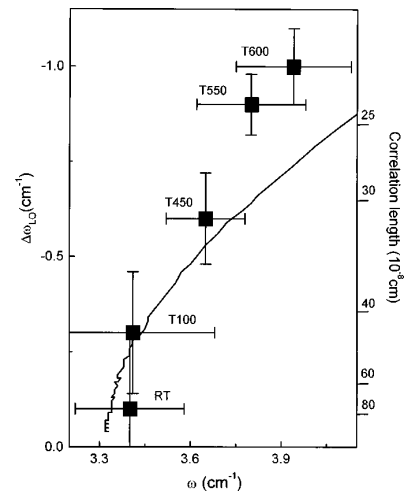


FIG. 4. The relationship between LO-phonon Raman shift $\Delta\omega_{\text{LO}}$ and broadening ω as a function of correlation length L_{cl} .

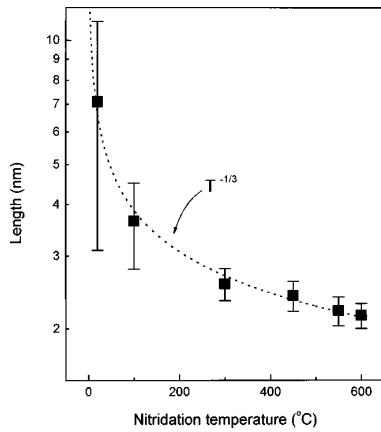


FIG. 5. The length L_N calculated with Eq. (7). The dotted line is the fitting proportional to $T^{-1/3}$, where T is the nitridation temperature.

(5) and (6). Thus the correlation length L_{cl} for each sample is estimated to be about 7.7 nm for RT and 2.2 nm for T600, respectively. As can be seen in Fig. 4, the theoretical value (solid line) agrees well with the experimental values of $\Delta\omega_{LO}$ and ω for the range of low nitridation temperature (lower than 450 °C) but differs slightly at high temperatures (higher than 550 °C). It seems that this difference may have originated from the theoretical calculation, which has neglected the effects of the point defects generated at high temperature.

Now, if we assume that defects, which are limited to only nitrogen atoms, are situated in the rectangular cell with the fraction x (%), then it means that one defect out of $100/x$ atoms in the cell of length L_N is situated at the center. So L_N is expressed as

$$L_N = (100/x)^{1/3}a, \quad (7)$$

where a ($=0.565$ nm) is the lattice constant of bulk GaAs. The length L_N calculated by substituting x into Eq. (7) is in the range from 2.0 to 7.2 nm as shown in Fig. 5 as a function of the nitridation temperature T . Here x is the value calculated from Eq. (4), and the dotted line of Fig. 5 is the fitting result that L_N is proportional to $T^{-1/3}$. From both fitting results of Figs. 3 and 5, we can conclude that as the nitridation temperature is raised up to 600 °C, the high degree of nitridation can be obtained while the disordering with respect to the correlation length tends to be saturated. The slight change of the length L_N at high temperature signifies a strong influence on the defects because of L_N being proportional to $T^{-1/3}$. Hence, comparing the estimated range of L_N with that of the correlation length L_{cl} , the agreement is quite good at the low nitridation temperature below 450 °C but there are some differences at the high temperature above 550 °C. This

means that the assumption for the defects limited to nitrogen atoms is valid at temperatures below 450 °C. However, some other defects should be considered additionally for the interpretation of the differences between L_{cl} and L_N at the high temperature above 550 °C. According to the analysis of the thin nitrided GaAs layer performed with DLTS (deep level transient spectroscopy) and XPS, the electron deep levels $N1$ ($E_c - 0.13$ eV) and $N2$ ($E_c - 0.58$ eV) associated with V_{As} related complexes such as $V_{As}-As_{Ga}$ and low energy ion beam induced defects, respectively, appeared in the samples treated at the high temperature above 450 °C.¹³ These point defects involved in the thin layer may result in disordering effects in Raman scattering measurement. Hence, the difference between the length L_N and the correlation length L_{cl} at the high temperature may be explained by the effects of the existence of the point defects such as V_{As} or $V_{As}-X$ complex in the nitrided thin layers where X may be As_{Ga} . Therefore, we may conclude that the fraction of nitrogen atoms is produced in proportion to the increasing nitridation temperature, but the point defects such as V_{As} or $V_{As}-X$ complex may be additionally generated at the high nitridation temperature above 550 °C.

IV. CONCLUSIONS

We have investigated several physical properties of the nitrided GaAs thin layer by Raman scattering. The observed Raman spectra in the nitrided sample have been interpreted by taking into account the change in lattice constant, the reduction in effective charge, and the relaxation of the \mathbf{q} -selection rule arising from the vanishing periodicity. The strain generated from the change in lattice constant affects TO and LO phonons equally, and the strain in the sample nitrided at 600 °C is estimated to be 0.15 GPa. It is also observed that the reduction in effective charge lessens the LO-TO splitting while increasing the nitridation temperature. Calculated from the LO-TO splitting, the fraction (x) of As sites substituted by N ranges from 0.05% to 1.8%. The fitting results show that the amount of the defects increases linearly with T , the nitridation temperature, whereas the length L_N is proportional to $T^{-1/3}$. The correlation length L_{cl} agrees well with the theoretical value in the range of low nitridation temperature below 450 °C but makes differences in some degree at the high temperature above 550 °C. By interpreting these differences, we have concluded that the point defects such as V_{As} or $V_{As}-X$ complex may be generated mainly at high nitridation temperature, while the fraction of nitrogen atoms involved in the thin nitrided GaAs layer increases in proportion to the nitridation temperature.

We acknowledge support by the BSRI program of MOE (Project No. BSRI-97-2410).

*Author to whom correspondence should be addressed. Electronic address: ekkoh@quanta.kbsi.re.kr

¹K. Uchida *et al.*, J. Appl. Phys. **79**, 3487 (1996).

²N. Koide *et al.*, J. Cryst. Growth **115**, 639 (1991).

³S. D. Nakamura *et al.*, Appl. Phys. Lett. **68**, 2105 (1996).

⁴S. Yoshida *et al.*, J. Cryst. Growth **136**, 37 (1994).

⁵M. E. Jones *et al.*, Appl. Phys. Lett. **67**, 542 (1995).

⁶S. Yoshida *et al.*, Surf. Sci. **267**, 50 (1996).

⁷P. Manuel *et al.*, Phys. Rev. Lett. **37**, 1701 (1976).

⁸B. Jusserand *et al.*, Solid State Commun. **48**, 499 (1983).

⁹G. Attolini *et al.*, J. Appl. Phys. **75**, 4156 (1994).

¹⁰H. Taino *et al.*, J. Appl. Phys. **70**, 7068 (1991).

¹¹P. Wickboldt *et al.*, Phys. Rev. B **35**, 1362 (1987).

¹²F. Cerderia *et al.*, Phys. Rev. B **5**, 580 (1972).

¹³Y. J. Park *et al.*, Appl. Surf. Sci. **117**, 551 (1997).

¹⁴H. Abe *et al.*, Jpn. J. Appl. Phys., Part 1 **35**, 5955 (1996).

¹⁵M. Calamitou *et al.*, Solid State Commun. **87**, 563 (1993).

¹⁶D. J. Evans and S. Ushioda, Phys. Rev. B **9**, 1638 (1974).

¹⁷T. A. Gant *et al.*, Appl. Phys. Lett. **60**, 1453 (1992).

¹⁸K. K. Tiong *et al.*, Appl. Phys. Lett. **44**, 122 (1984).

¹⁹P. Paryanthal and F. H. Pollak, Phys. Rev. Lett. **52**, 1822 (1984).